Available online at www.sciencedirect.com
ScienceDirect
European Journal of Medicinal Chemistry 43 (2008) 1506–1518
EUROPEAN JOURNAL OF MEDICINAL CHEMISTRY
http://www.elsevier.com/locate/ejmech

Original article

Synthesis and in vitro biological evaluation of valine-containing prodrugs derived from clinically used HIV-protease inhibitors

Dominique Roche [a], Jacques Greiner [a], Anne-Marie Aubertin [b], Pierre Vierling [a,*]

[a] *Laboratoire de Chimie des Molécules Bioactives et des Arômes, UMR 6001, Université de Nice Sophia-Antipolis, CNRS, Faculté des Sciences, Institut de Chimie de Nice, 28, avenue de Valrose, 06100 Nice, France*
[b] *INSERM U74, Institut de Virologie, 3 rue Koeberlé, 67000 Strasbourg, France*

Received 23 April 2007; received in revised form 13 July 2007; accepted 9 August 2007
Available online 14 September 2007

Abstract

In an approach to improve the pharmacological properties and pharmacokinetic profiles of the current protease inhibitors (PIs) used in clinics, and consequently, their therapeutic potential, we performed the synthesis of PI–spacer–valine prodrugs (PI = saquinavir, nelfinavir and indinavir; spacer = $-C(O)(CH_2)_5NH-$), and evaluated their in vitro stability with respect to hydrolysis, anti-HIV activity, cytotoxicity, and permeation through a monolayer of Caco-2 cells (used as a model of the intestinal barrier), as compared with their parent PI and first generation of valine–PIs (wherein valine was directly connected through its carboxyl to the PIs). The PI–spacer–valine conjugates were prepared in two steps, in good yields, by condensing an acid derivative of the appropriate protected valine–spacer moiety with the PI, followed by deprotection of the valine protecting group. With respect to hydrolysis, we found that the PI–spacer–valine prodrugs were chemically more stable than the first generation of PI–Val prodrugs. Their stabilities correlated with the low to very low in vitro anti-HIV activity measured for those prodrugs wherein the coupling of valine–spacer residue to the PIs was performed onto the peptidomimetic PI's hydroxyl. Prodrugs wherein the coupling of the valine–spacer residue was performed onto the non-peptidomimetic PI hydroxyl displayed a higher antiviral activity, indicating that these prodrugs are also to some extent anti-HIV drugs by themselves. While the direct conjugation of L-valine to the PIs constituted a most appealing alternative, which improved their absorptive diffusion across Caco-2 cell monolayers and reduced their recognition by efflux carriers, its conjugation to the PIs through the $-C(O)(CH_2)_5NH-$ spacer was found to inhibit their absorptive and secretory transepithelial transport. This was attributable to a drastic reduction of their passive permeation and/or active transport, indicating that the PI–spacer–valine conjugates are poor substrates of the aminoacid carrier system located at the brush border side of the Caco-2 cell monolayer.

Keywords: HIV-protease inhibitors; Valine-containing prodrugs; Saquinavir; Indinavir; Nelfinavir; Transport; Caco-2 monolayer

1. Introduction

Highly active antiretroviral therapies (HAART) against AIDS-HIV infection using a combination of HIV reverse transcriptase and protease inhibitors have been remarkably successful, leading to a decline in morbidity and mortality [1,2]. However, despite these HAARTs, viral replication is still persisting, indicating, among others, the existence of reservoirs or sanctuaries for the virus, such as the lymphatic system and central nervous system [3–5], wherein the antivirals, and more particularly the protease inhibitors (PIs), do not penetrate at an efficient inhibitory level [6,7]. Most of these PIs display disadvantageous physicochemical and pharmacological properties. To overcome their suboptimal pharmacokinetics, high daily doses must be ingested, often with food and fluid restrictions. This complicates patient adherence, and contributes to resistance issues and to the appearance of serious long-term metabolic complications, such as cardiovascular disturbances, hyperlipidemia, lipodystrophy, insulin resistance, osteopenia, and diabetes [8–12], and to lower the viral

* Corresponding author. Tel.: +33 4 92 07 61 43; fax: +33 4 92 07 61 51.
E-mail address: vierling@unice.fr (P. Vierling).

0223-5234/$ - see front matter © 2007 Elsevier Masson SAS. All rights reserved.
doi:10.1016/j.ejmech.2007.08.016

treatment outcome [13]. In order to reduce viral replication in infected patients, an alternative is to improve the pharmacological properties, safety and pharmacokinetic profiles, and, consequently, the therapeutic potential of the PIs already used in clinics. Aiming at this goal, we [14–20] and others [21–31] adopted the very efficient prodrug approach. Successful results were obtained with the disclosure of the FDA approved fosamprenavir, a phosphate ester prodrug of amprenavir [32–36]. However, a number of shortcomings have still to be overcome for the PIs. Among others, the generation of PI prodrugs should display higher water solubility, increased bioavailability (plasma concentration, blood circulation time), and/or improved delivery of the parent PI into HIV sanctuaries. One should therefore be able with these PI prodrugs to (i) circumvent drug inactivation resulting from their in vivo binding to plasma proteins, (ii) limit their rapid metabolization and inactivation by cytochrome P450 3A4, and/or (iii) inhibit their possible transport by the multidrug-resistant P-glycoprotein (P-gp) responsible for their limited oral bioavailability and brain penetration [13,37].

In our previous studies [14–20], and with the aim of improving drug permeation through the intestinal and blood brain barrier by targeting influx carrier-mediated transport systems, we designed PI–aminoacid ester prodrugs. The benefit of this approach was shown for increasing their permeation across polarized monolayers formed of the human intestinal Caco-2 cells (which are widely approved models of the intestinal epithelium). Among many tested compounds, the ester Ind(8)–Val (see structure in Fig. 1) exhibited extended stability with respect to hydrolysis and a dramatic improvement of permeation characteristics compared to the parent compound (Fig. 1) [16,18]. Ind(8)–Val was therefore selected as an interesting candidate for further in situ and in vivo investigations in an attempt to characterize both its oral bioavailability and CNS distribution. Unfortunately, its promising biopharmaceutical characteristics suggested from the in vitro experiments were not confirmed by the in situ and in vivo experiments [19]. Apart from Ind(8)–Val, most of these PI–aminoacid ester compounds released the active free drug very rapidly (half-lives of hydrolysis in buffer at 37 °C of 3–4 h) while their carbamate analogs were too stable, thus hampering further in vivo developments [15,18].

In continuation with this work, we designed the PI–spacer–aminoacid prodrugs wherein L-valine and the PI are tethered together with a $-C(O)(CH_2)_5NH-$ spacer. The spacer was introduced for the modulation of the chemical and biological stability of the prodrugs, and for the accessibility of valine, thus allowing a better recognition by its cellular transporters. To preserve its recognition by the aminoacid transporter systems, valine was conjugated via its acid function to the amine function of the spacer unit, which, via its acid extremity, was linked to the PI through a hydrolyzable ester function. As esterases are ubiquitous in cells, in vivo hydrolysis of the ester prodrugs is expected to release the active parent drug [38]. Such a spacer strategy proved very successful for increasing the resistance to hydrolysis of the

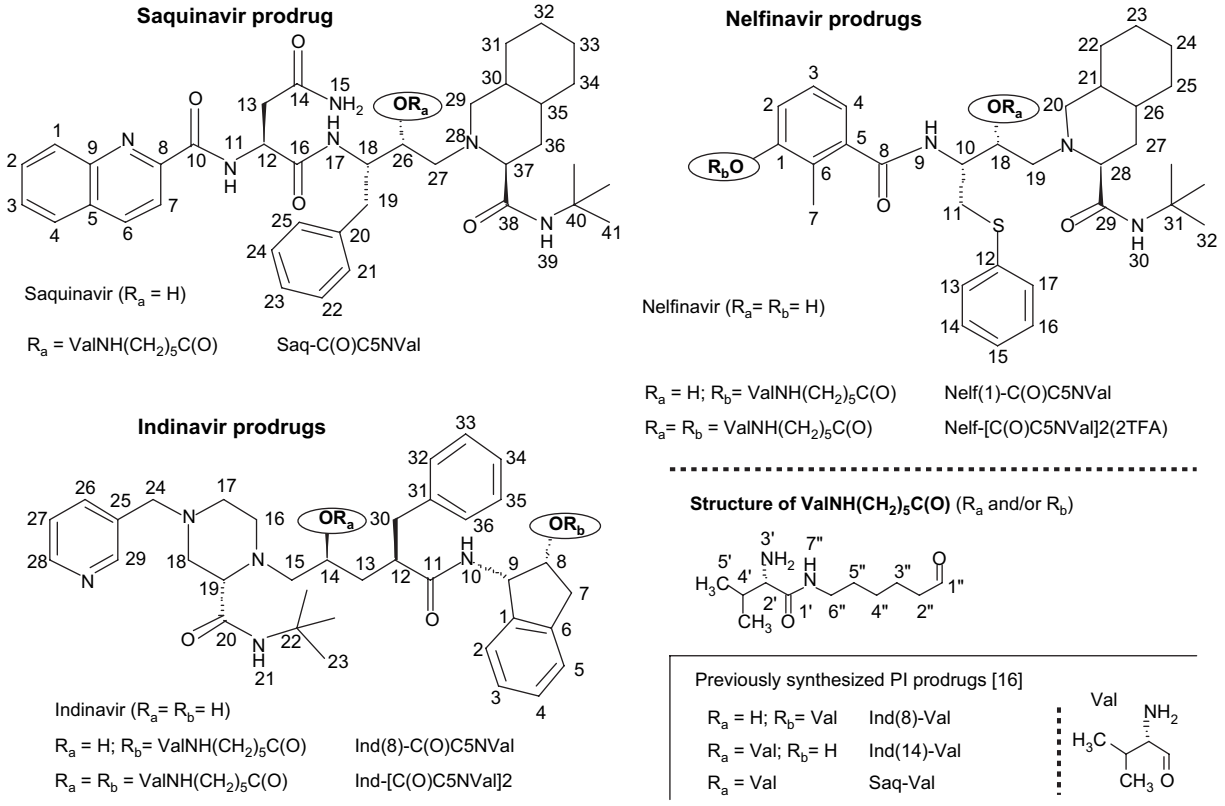

Fig. 1. Chemical structures and code names of the valine-containing protease inhibitor (PI = saquinavir, indinavir, and nelfinavir) prodrugs described in this study and atom numbering used in the description of their NMR spectra.

highly unstable PI–tyrosine conjugates [14,18]. However, its impact on the pharmacological properties could therefore not been evaluated.

This paper is dedicated to the synthesis of various PI–spacer–valine prodrugs (Fig. 1), their chemical stability with respect to hydrolysis under physiological conditions, and their in vitro anti-HIV activity. Using the well-known Caco-2 intestinal barrier model, we report also on their transepithelial transport. All these features are some of the prerequisites for further in vitro and in vivo investigations.

2. Chemistry

The PI–spacer–valine prodrugs shown in Fig. 1 were prepared in two steps by condensing saquinavir, indinavir or nelfinavir with the key (*N*-Boc)-valine–spacer acid synthon **1**, followed by deprotection of the amino protecting group (Scheme 1). Synthon **1** was obtained by condensing 6-aminohexanoic acid with *N*-Boc-(L)-Val in the presence of HOSu/DCC (75% yield [39]).

Concerning saquinavir, acylation of its unique hydroxyl was performed in nearly 70% yield using conventional EDC/DMAP as coupling reagent [40]. Concerning indinavir and nelfinavir, both of which contain two hydroxyls, and in line with previous work [14,15,18,20], a stochastic esterification – one to one equivalent – was preferred instead of a more tedious and time-consuming protection/deprotection strategy (though more elegant and probably more efficient in terms of yields) of one of these two hydroxyls. The stochastic esterification led into the formation of a mixture of mainly the monoester and diester resulting from the acylation of the C1-hydroxyl of nelfinavir (30% yield) and C8-hydroxyl of indinavir (20% yield), and of both hydroxyls (10% yield for nelfinavir and 18% yield for indinavir), respectively (for the atom numbering, see Fig. 1). Only traces of the monoester corresponding to the acylation of the C18-hydroxyl of nelfinavir and C14-hydroxyl of indinavir were detected by TLC.

Deprotection of the *N*-Boc protecting group in the saquinavir, indinavir or nelfinavir conjugates was achieved in a 1:9 TFA/CH_2Cl_2 medium and afforded in 87–100% yields the target Saq–C(O)C5NVal (isolated as its tri-TFA salt), Ind(8)–C(O)C5NVal (isolated as its mono-TFA salt), Ind–[C(O)C5Val]2 (isolated as its di-TFA salt), Nelf(1)–C(O)C5Val (isolated as its mono-TFA salt), and Nelf–[C(O)C5Val]2 (isolated as its di-TFA salt) prodrugs, respectively. The TFA anion quantification in the isolated materials was assessed by ^{19}F NMR using 3,3,3-trifluoroethanol as internal standard.

The chemical structures of all protected and deprotected PI prodrugs were unambiguously ascertained by ^{1}H, ^{13}C NMR and mass spectrometry. That the isolated monoesters resulted from the selective acylation of the C-26 saquinavir, C-8 indinavir and C-1 nelfinavir hydroxyls, respectively, was attested more particularly by ^{1}H and ^{13}C NMR. As expected, the resonances of the corresponding H-26 proton and C-26 carbon atoms of the saquinavir derivatives were shifted downfield [$|\Delta| = 1.25 - 1.36$ ppm and $|\Delta| = 6.6 - 7.3$ ppm, respectively] in comparison with those of saquinavir [δ(H-26) = 3.95 ppm; δ(C-26) = 67.1 ppm]. For indinavir, acylation at the C-8 position (as in Ind(8)–C(O)C5N(Boc)Val) was evidenced by the downfield shift of the H-8 ($|\Delta| = 1.10 - 1.18$ ppm) and C-8 carbon resonance ($|\Delta| = 3.0 - 3.8$ ppm), and the upfield shift of the vicinal C-9 carbon signal (see Table 1). Furthermore, that the H-14/C-14 and C-13/15 vicinal β-carbon resonances of indinavir and Ind(8)–C(O)C5N(Boc)Val were located at very close chemical shifts indicated that the C-14 hydroxyl group was not acylated [41,42]. By contrast, when esterification of the indinavir C-14 position (as in Ind–[C(O)C5N(Boc)Val]2) had occurred, a significant downfield shift of the H-14/C-14 atom resonances and upfield shift of the C-13/15 vicinal β-carbon ones was observed, as expected (see Table 1). For nelfinavir, acylation of only its aromatic C-1 hydroxyl (as in Nelf(1)–C(O)C5N(Boc)Val) was highlighted by the shielding ($|\Delta| = 5.7$ ppm) of the C-1 carbon signal and the concomitant deshielding of its C-2/6 vicinal β-carbon atoms (by about 8 and 6 ppm), as expected for phenyl esters. That the remaining C-18 hydroxyl of Nelf(1)–C(O)C5N(Boc)Val was not substituted was further supported by the H/C-18 and C-10/19 vicinal resonances, which appeared at very close chemical shifts to those of nelfinavir (see Table 1) [43,44]. Its esterification (as in Nelf–[C(O)C5N(Boc)Val]2) was unambiguously confirmed by the downfield shift of the H-18 signal from 3.98 ppm (for free nelfinavir) to 5.36 ppm for the diester prodrug, and of C-10/19 vicinal resonances, though the C-18 chemical shift remains almost unaffected (see Table 1). All these data are further in line with those reported for the C-8/C-14 indinavir and C-1/C-18 nelfinavir prodrugs [14,15,18,20].

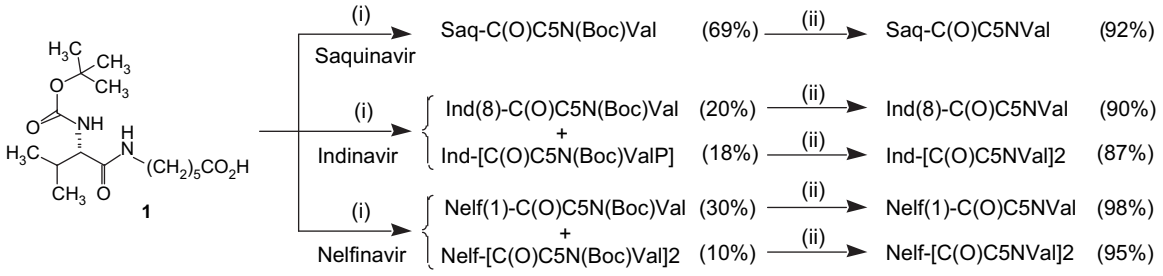

Scheme 1. Synthetic pathway to the PI–spacer–valine prodrugs (PI = saquinavir, indinavir, and nelfinavir; spacer = $-C(O)(CH_2)_5NH-$): (i) EDC/DMAP, CH_2Cl_2 (or DMF); (ii) TFA, CH_2Cl_2. All the deprotected prodrugs were isolated as TFA salts. For more details, see Section 6.

Table 1
^{13}C chemical shifts of the indinavir C-8/14, nelfinavir C-1/18 carbon atoms bearing a hydroxyl or an acyl functionality, and of their vicinal carbon atoms (C-β) (for the atom numbering, see Fig. 1)

Compound	^{13}C chemical shifts (in ppm)					
	C-14	C-13 (β)	C-15 (β)	C-8	C-7 (β)	C-9 (β)
Indinavir	65.8	39.2	61.5	73.0	38.1	57.5
Ind(8)–C(O)C5N(Boc)Val	66.2	38.8	61.6	76.0	37.6	55.1
Ind(8)–C(O)C5NVal	67.1	40.6 or 40.3	62.6	76.8	38.2	56.7
Ind–[C(O)C5N(Boc)Val]2	69.8	37.5	58.9	75.8	39.0	55.2
Ind–[C(O)C5NVal]2	69.5	37.1	58.3	75.6	38.7	55.0

Compound	^{13}C chemical shifts (in ppm)					
	C-18	C-10 (β)	C-19 (β)	C-1	C-6 (β)	C-2 (β)
Nelfinavir	70.5	54.2	59.6	156.8	123.4	116.8
Nelf(1)–C(O)C5N(Boc)Val	70.7	54.7	59.8	151.1	129.6	124.7
Nelf(1)–C(O)C5NVal	70.4	54.4	59.6	151.1	129.4	124.6
Nelf–[C(O)C5N(Boc)Val]2	70.5 or 70.3	51.3	55.9	149.6	128.2	123.2
Nelf–[C(O)C5NVal]2	72.1	51.7	57.8	151.2	129.3	124.9

3. Pharmacology

The in vitro stability of synthesized saquinavir, nelfinavir and indinavir prodrugs with respect to hydrolysis (expressed by their hydrolysis half life ($t_{1/2}$)) was checked using the same hydrolysis protocol as that described in previous studies from our laboratory [14]. These experiments were performed in a pH 7.3 buffer at 37 °C and in the absence of serum, cells and virus using a prodrug concentration in the 0.26–1.85 mM range which necessitated the addition of 2–5% (v/v) of MeOH to the medium. The HIV inhibition levels (IC_{50}) and cytotoxicities (CC_{50}) of the valine–spacer saquinavir, indinavir, and nelfinavir conjugates (as their TFA salt) were evaluated in vitro in CEM-SS and MT-4 cell cultures infected with HIV-1 LAI and HTLV IIIB, respectively, according to published procedures [45–47]. All these data are collected in Table 2 together with those of their parent PIs [14,48] and first generation of PI–Val prodrugs [14].

Their permeation was assessed in vitro through a monolayer of Caco-2 cells used as an intestinal barrier model, according to the same protocol employed previously [14]. The results of the bi-directional transport studies of the various PI–spacer–valine prodrugs and of their parent PI are presented in Fig. 2 (which illustrates the transport profiles) and Table 3 (which collects the percentages of transported (pro)drug and the apparent permeability coefficients P_{app} calculated from the slope of a plot of the cumulative receiver concentration with time).

4. Results and discussion

4.1. Biological activity and chemical stability

The saquinavir hydroxyl, the indinavir C-14 but not the C-8 hydroxyl, and the nelfinavir C-18 but not the C-1 hydroxyl, are involved in the peptidomimetic noncleavable transition state isostere responsible for the protease inhibitory potency of saquinavir, indinavir, and nelfinavir, respectively [49]. Therefore, it is most important that these hydroxyls be accessible for antiviral activity. In the previous studies dedicated to the ester prodrugs of saquinavir, indinavir and nelfinavir [14,18], a close correlation between their anti-HIV activity and the hydrolysis of their acylated "peptidomimetic" hydroxyl, hence the liberation of the active free drug during the time of incubation, was found: the faster the hydrolysis, the closer the anti-HIV activity level to that of the respective parent drug. Concomitantly, the level of HIV inhibition was very low for the prodrugs for which hydrolysis and release of this

Table 2
Anti-HIV activity (IC_{50}) and cytotoxicity (CC_{50}) data for saquinavir, indinavir and nelfinavir prodrugs in CEM-SS and MT-4 cell cultures infected with HIV-1 LAI and HTLV IIIB, respectively, together with their hydrolysis half life ($t_{1/2}$)

Compound[a]	IC_{50} (nM) CEM-SS	R[b]	IC_{50} (nM) MT4	R[b]	CC_{50} (M) CEM-SS	CC_{50} (M) MT4	$t_{1/2}$[c] (h)
Saquinavir[h]	9	–	18	–	$>10^{-5}$	$>10^{-5}$	–
Saq–Val[e]	140	16	290	16	$>10^{-5}$	$>10^{-5}$	40
Saq–C(O)C5NVal	175	19	340	19	9×10^{-6}	53×10^{-7}	60
Indinavir[g]	≤10	–	22	–	$>10^{-4}$	$>10^{-4}$	–
Ind(8)–Val[e]	17	≥1.7	150	7	$>10^{-4}$	$>10^{-4}$	46[f]
Ind(14)–Val[e]	90	≥9	27	~1	$>10^{-4}$	$>10^{-4}$	68
Ind(8)–C(O)C5NVal	36	≥3.6	230	10	$>10^{-5}$	4.7×10^{-5}	72
Ind–[C(O)C5NVal]2	640	≥64	2950	134	$>5 \times 10^{-5}$	4.5×10^{-5}	80
Nelfinavir[h]	2[d]	–	–	–	–	–	–
Nelf(1)–C(O)C5NVal	94	47	230		$>10^{-5}$	$>10^{-5}$	72
Nelf–[C(O)C5NVal]2	15,500	7750	$>CC_{50}$		5×10^{-6}	4.8×10^{-6}	82

[a] Prodrugs were used as their TFA salt; see Fig. 1 for the structures of valine-derived prodrugs.
[b] R is the ratio of the prodrug IC_{50} to that of its parent compound.
[c] $t_{1/2}$, which corresponds to the time at which 50% of hydrolysis is observed (measurement of disappearance of the prodrug), has been determined from hydrolysis experiments performed by incubating the prodrugs in a pH 7.3 DMEM solution at 37 °C.
[d] Data from Ref. [48].
[e] Data from Ref. [14].
[f] Data from Ref. [18].
[g] Used as its sulfate.
[h] Used as its mesylate salt.

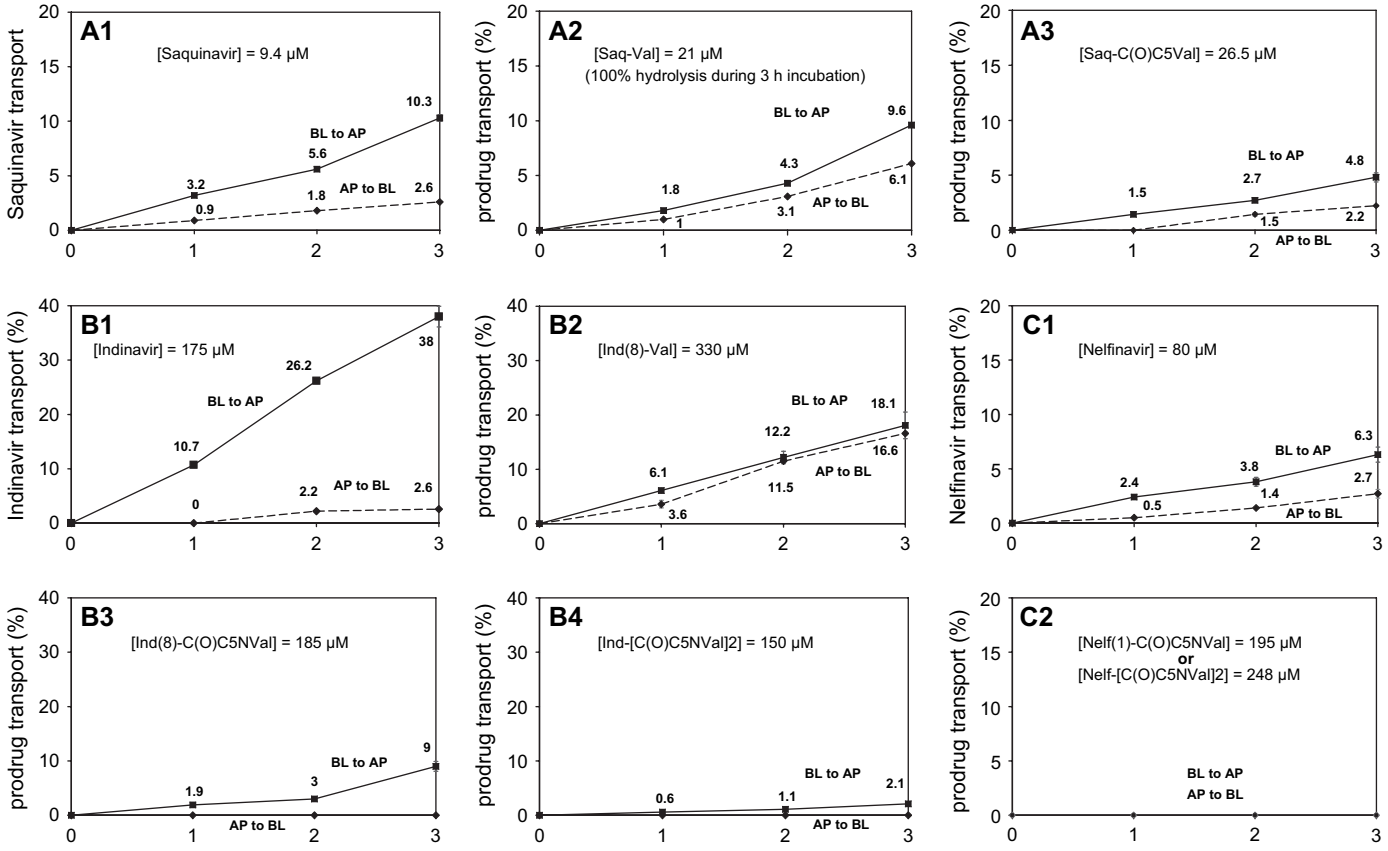

Fig. 2. Bi-directional transepithelial transport across a Caco-2 cell monolayer of PI–spacer–valine-conjugates (panels A3, B3-4, C2) in comparison with that of their parent drugs (panels A1, B1, C1) and/or PI–Val conjugates (panels A2, B2) (data from Ref. [16]). Absorptive translocation [apical (AP) to basolateral (BL) compartment]: *lozenges*. Secretory translocation (BL to AP): *squares*. The results are expressed as (pro)drug transport percentages (%) vs time (in hours). The percentage values represent the ratios of (pro)drug concentration in receiver vs donor chamber × 100. The initial concentration of the (pro)drug in the donor compartment is indicated on each panel. Results are means ± SD from three experiments. All incubations were performed at 37 °C and pH 7.4.

Table 3
Log *P* data of the PIs and prodrugs, their percentages of (pro)drug transport from the donor chamber after the 3 h of experiment, and apparent permeability coefficients P_{app}

Compound[a] [concentration in donor chamber (μM)]	Log *P*[d]	BL to AP		AP to BL	
		% (±SD) in receiver	P_{app} (±SD) (cm/s, ×1E − 8)	% (±SD) in receiver	P_{app} (±SD) (cm/s, ×1E − 8)
Saquinavir [9.4][f]	4.727 (4.73)[e]	10.3 (1.9)	398 (117)	2.6 (0.4)	110 (31)
Saq–Val[b,c] [21]	5.963	9.6 (0.1)	343 (22)	6.1 (0.3)	232 (22)
Saq–C(O)C5NVal [26.5]	6.182	4.8 (0.4)	187 (24)	2.2 (0.1)	58 (8)
Indinavir [175][g]	3.681 (3.68)[e]	38 (2)	1550 (234)	2.6 (0.3)	103 (10)
Ind(8)–Val[b] [330]	4.923	18.1 (0.3)	737 (26)	15.6 (0.4)	644 (44)
Ind(14)–Val[b] [177]	4.891	14.6 (0.5)	708 (147)	14.0 (0.4)	513 (50)
Ind(8)–C(O)C5NVal [185]	5.141	9 (0.9)	292 (17)	nd	–
Ind–[C(OC5NVal]2 [150]	6.531	2.1 (0.2)	625 (86)	nd	–
Nelfinavir [80][f]	5.842 (5.84)[e]	6.3 (1.4)	251 (68)	2.7 (1.1)	103 (66)
Nelf(1)–C(O)C5NVal [195]	6.377	nd	–	nd	–
Nelf–[C(O)C5NVal]2 [248]	7.436	nd	–	nd	–

nd = not detected, i.e. below the detection limit which is 0.4, 0.1, and 0.1 μM for the indinavir, saquinavir, and nelfinavir derivatives, respectively.

[a] Prodrugs were used as their TFA salts; see Fig. 1 for the structures of valine-derived prodrugs.

[b] Data from Ref. [16].

[c] 100% hydrolysis during 3 h experiment (for more details, see Section 6).

[d] Calculated using Chem 3D Ultra 8.0, CambridgeSoft, Cambridge, MA.

[e] Data taken from Ref. [60] and calculated using CQSAR program.

[f] Used as its mesylate salt.

[g] Used as its sulfate.

peptidomimetic hydroxyl was very slow. On the other hand, no correlation was found between the hydrolysis rate of the acylated C-8 indinavir prodrugs (C-8 hydroxyl is not part of the transition state isostere) and their anti-HIV activity [14].

All the valine–spacer prodrugs, when incubated in the same conditions (pH 7.3 buffer at 37 °C and in the absence of serum, cells and virus) as the first generation of PI–Val prodrugs, were hydrolyzed within a close interval of time, their hydrolysis $t_{1/2}$ being comprised between 60 and 82 h (Table 2). As compared with the chemical stability of the PI–Val prodrugs, the PI–C(O)C5NVal conjugates displayed a 50–60% improved resistance to hydrolysis, which can be attributed to the presence of the $-C(O)(CH_2)_5NH-$ spacer. These results are in line with those established for tyrosine–PI prodrug analogs containing a $-C(O)(CH_2)_4-$ spacer linking the PI to the tyrosine hydroxyl [18].

In line with previous studies, the anti-HIV efficiency of saquinavir, indinavir, and nelfinavir was substantially reduced upon conjugation of the valine–spacer moiety to the peptidomimetic hydroxyl of these PIs (as in Saq–C(O)C5NVal, Ind–[C(O)C5Val]2 and Nelf–[C(O)C5Val]2) as well as to the hydroxyl of indinavir and nelfinavir, which is not part of the transition state isostere (as in Ind(8)–C(O)C5NVal, Nelf(1)–C(O)C5NVal). This is illustrated by the R values (from $\geq$3.6 to 7750), which correspond to the ratio of the IC_{50} of the PI prodrug vs that of the parent PI (see Table 2). The lower anti-HIV activities of these PI prodrugs reflect to some extent their relative stabilities with respect to hydrolysis during the 5-day time-span of the antiviral assays. In line with previous studies, we found also a correlation between antiviral activity and chemical stability, the most active prodrug in a given series (i.e. Saq–Val vs Saq–C(O)C5NVal and Ind(8)–Val vs Ind(8)–C(O)C5NVal) being the less stable one (hence Saq–Val and Ind(8)–Val).

It should further be emphasized that the Ind(8)–valine and Nelf(1)–valine conjugates can be seen not only as prodrugs but also as potential anti-HIV drugs. Indeed, the C-8 hydroxyl of indinavir and C-1 hydroxyl of nelfinavir (onto which the valine–spacer unit was conjugated) are not involved in the noncleavable transition state isostere responsible for their protease inhibitory potency. Their hiding (as in Ind(8)–Val, Ind(8)–C(O)C5NVal, Nelf(1)–Val, Nelf(1)–C(O)C5NVal) should therefore not modify drastically the antiviral activity of indinavir and nelfinavir, respectively. This was indeed what was found for the indinavir conjugates, which display an antiviral activity slightly lower to that of indinavir ($R \sim 3.6$–10). However, masking of the ''non-peptidomimetic'' C-1 hydroxyl of nelfinavir decreased more significantly the antiviral activity of nelfinavir ($R \sim 47$ for Nelf(1)–C(O)C5NVal). These data indicate likely that (i) these conjugates themselves may possess an antiviral activity, which is lower than that of their parent drug, and/or (ii) the connection of the L-valine substituents onto this non-peptidomimetic hydroxyl reduces the recognition by the protease, thus decreasing the interactions between the peptidomimetic noncleavable isostere and viral protease active site. This phenomenon also accounts, in part, for the very low anti-HIV activity of the indinavir- and nelfinavir-diester derivatives. It is further noteworthy that no cytotoxicity was detected for any of these prodrugs.

4.2. Transepithelial transport

There is currently a considerable interest in increasing the absorptive permeability of the HIV PIs and reducing their secretion by the efflux carrier systems, such as the multidrug-resistant P-glycoprotein (P-gp) which is responsible for their limited oral bioavailability and brain penetration [50,51]. In this regard, esterase-rich and efflux carrier-expressing Caco-2 cell line monolayers are widely accepted in vitro models of the intestinal epithelium for screening drug and prodrug candidates and thus for evaluating prodrug approaches for enhanced intestinal drug absorption [52–56]. Caco-2 cell line monolayers have already been used in numerous studies to characterize the permeation of various (pro)drugs, including indinavir, saquinavir, nelfinavir [50,51,57,58], and those prodrugs, which have been developed in our laboratory [16,18,20].

Translocation of the various valine–spacer–PI prodrugs across the polarized Caco-2 cell monolayers was evaluated at a concentration where they are soluble and in comparison with that of their parent PI and first generation of Val–PIs. Investigation of the transport across the cell monolayer in the absorptive [from apical (AP) to basolateral (BL)] and secretory (from BL to AP) directions constitutes a mean of evaluating the influence of P-gp and related efflux carriers, which are located on the AP side of the monolayer. Transepithelial electrical resistance after confluence has been used to monitor the integrity of the cell monolayer [59]. Translocation was initiated by adding the test solution to the AP or BL side of the monolayer (donor chamber). As Caco-2 cells are also rich in esterases, the hydrolysis of the ester prodrugs during their permeation across the monolayer was carefully checked. Only the prodrugs were detected either in the donor or acceptor chamber, indicating that no hydrolysis had occurred after the 3 h of transport experiments.

Most importantly, the transport results (Fig. 2 and Table 3) indicate that conjugation of L-valine to the PIs through a spacer, as in the PI–C(O)C5NVal conjugates, had detrimental effects on PI permeation across the Caco-2 cell monolayer, by contrast with its direct conjugation, as in Saq–Val, Ind(8)–Val and Ind(14)–Val, which was most beneficial. Indeed, in the adsorptive AP to BL direction and in the saquinavir series, a nearly 3-fold translocation decrease was measured for Saq–C(O)C5NVal (Fig. 2, panel A3) as compared with Saq–Val (Fig. 2, panel A2), permeation of Saq–C(O)C5NVal being further comparable with that of its parent saquinavir (Fig. 2, panel A1). No transport at all was detected neither for Ind(8)–C(O)C5NVal (Fig. 2, panel B3) nor for Nelf(1)–C(O)C5NVal (Fig. 2 panel C2), at least above the detection limit for those derivatives, whereas a substantial (5- to 6-fold) improvement of indinavir permeation was noticed with Ind(8)–Val (Fig. 2, panel B2) and Ind(14)–Val (not shown) [16]. In the secretory BL to AP direction, a significantly larger reduction

of permeation of the PIs was also found for the PI–C(O)C5NVal prodrugs as compared with the PI–Val conjugates. In comparison with that of its parent drug, secretory efflux of Saq–C(O)C5NVal (respectively Ind–C(O)C5NVal) was 2-fold (respectively 6-fold) lower, whereas that of Saq–Val (respectively Ind–Val) was similar (respectively only 2- to 3-fold lower).

These substantial PI absorptive and secretory transport decreases resulting from the conjugation of valine to the PIs through the $-C(O)(CH_2)_5NH-$ spacer are attributable to a drastic reduction of either (i) the active transport, indicating that the PI–C(O)C5NVal conjugates are, as compared to the PI–Val conjugates, poor substrates of the aminoacid carrier system located at the brush border side of the Caco-2 cell monolayer, and/or (ii) more likely the passive permeation. It can also be assigned to an increase of affinity of the apically localized efflux P-gp carriers for those PI–C(O)C5NVal conjugates, as supported by their asymmetric permeation profile [50,51]. Moreover, the lower secretory transport for the valine–spacer–PI conjugates as compared to that of their parent PI and PI–Val conjugates indicates further that conjugation of the valine–spacer moiety to the PIs reduces their passive permeation to a larger extent than the direct conjugation of valine. However, the decrease of passive permeation is not reflected by the resulting increase of lipophilicity when going from the PIs, to the PI–Val conjugates then to the PI–spacer–Val derivatives, as expressed by the increase of their log *P* coefficient (Table 3).

Such poor absorptive and secretory transport profiles were also observed for PI–spacer–tyrosine conjugates [18]. However, it could not be attributed to the presence of the spacer unit as the PI–tyrosine derivatives were too unstable to allow transport experiments to be performed.

5. Conclusion

This study, aimed at improving the pharmacological properties and pharmacokinetic profiles of the PIs and of their first generation of valine–PI prodrugs wherein valine (through its carboxyl) was directly connected to the PIs, was dedicated to the synthesis of PI–spacer–valine prodrugs (PI = saquinavir, indinavir, and nelfinavir; spacer = $-C(O)(CH_2)_5NH-$), and the evaluation of their chemical stability, anti-HIV activity, and permeation across monolayers of Caco-2 cells as models of the intestinal barrier. The PI–spacer–valine conjugates were prepared in two steps, in good yields, by condensing an acid derivative of the appropriate protected valine–spacer moiety with the PI, followed by deprotection of the valine protecting group. With respect to hydrolysis, we found that these PI–spacer–valine prodrugs are chemically more stable than the first generation PI–Val prodrugs. Their chemical stabilities with half-life times in the 60–82 h range are further compatible with an in vivo utilization aimed at improving the absorption/penetration or accumulation of the prodrug in specific cells/tissues and liberation of the active free drug.

These stabilities correlate with the low to very low in vitro anti-HIV activity measured for those prodrugs wherein the coupling of valine–spacer residue to the PIs was performed onto the peptidomimetic PI's hydroxyl (as in Saq–C(O)C5NVal, Ind–$[C(O)C5NVal]_2$ and Nelf–$[C(O)C5NVal]_2$). Ind(8)–C(O)C5NVal and Nelf(1)–C(O)C5NVal prodrugs wherein the coupling of the valine–spacer residue was performed onto the non-peptidomimetic PI hydroxyl displayed a higher antiviral activity, indicating that these prodrugs are also to some extent anti-HIV drugs by themselves.

While the conjugation of L-valine (through its carboxyl) to the PIs constituted a most appealing alternative, which improved their absorptive diffusion across Caco-2 cell monolayers used as a model of the intestinal barrier, and reduced their recognition by efflux carriers, its conjugation to the PIs through the $-C(O)(CH_2)_5NH-$ spacer was found to inhibit their absorptive and secretory transepithelial transport. This was attributable to a drastic reduction of their passive permeation and/or active transport, indicating that the PI–spacer–valine conjugates are poor substrates of the aminoacid carrier system located at the brush border side of the Caco-2 cell monolayer.

6. Materials and methods

6.1. Chemistry

6.1.1. General methods, reagents and starting materials

All the reactions were performed under anhydrous nitrogen using dry solvents and reagents. Anhydrous solvents were prepared by standard methods. *N*,*N*′-Dicyclohexylcarbodiimide (DCC), 1-(3-dimethylaminopropyl)-3-ethyl-carbodiimide hydrochloride (EDC), 4-dimethylaminopyridine (DMAP), *N*-hydroxysuccinimide (HOSu) were purchased from Aldrich, and 6-aminohexanoic acid, *N*-Boc-L-valine, and trifluoroacetic acid (TFA) from Fluka. All these materials were used without further purification. Saquinavir, indinavir and nelfinavir (as their methanesulfonate salt or sulfate salt) were a gift from Hoffmann-La Roche, E. Merck, and Agouron, respectively, and were deprotonated prior to their use in the synthetic processes ($CHCl_3$ or EtOAc extraction of the free base from a $NaHCO_3$ or Na_2CO_3 10% solution of the protease inhibitor).

Column chromatography purifications were carried out on Silica Gel 60 (E. Merck, 70–230 mesh). The purity of all new compounds was checked by TLC, NMR, MS and HPLC. TLC analyses were performed on precoated Silica Gel F254 plates (E. Merck) with detection by UV and ninhydrin. HPLC analyses of the synthesized prodrugs (flow of 1 mL/min) were performed using a HP1100 apparatus using a Lichrospher 100 RP-18 (5 μm) column (250 × 3.2 mm) with gradient A: H_2O–CH_3CN (v:v) 0.1% TFA gradient as eluent (from 80:20 to 0:100) over 30 min; UV detection at 210 nm. With these conditions, retention times (t_R) of indinavir, nelfinavir, and saquinavir are of 10.4, 10.8, and 15.3 min, respectively. ^1H, ^{13}C, and ^{19}F NMR spectra were recorded with a Brucker AC 200 or AC 500 spectrometer at 200 (or 500), 50.3 (or 125.8), and 188.3 MHz, respectively.

^{19}F NMR with 3,3,3-trifluoroethanol as internal standard was used to assess the TFA anion quantification in the isolated valine-deprotected target compounds. Chemical shifts (δ) are given in ppm with respect to tetramethylsilane measured indirectly (i) to $CHCl_3$ (δ 7.27) for ^{1}H and (ii) to $CDCl_3$ (δ 76.9) for ^{13}C. Concerning the description of the prodrug NMR spectra, the atoms of the PI part are depicted as C-*x* and H-*y* whereas those of the valine part are depicted as C-*x*′ and H-*y*′ and those of the linker part are depicted as C-*x*″ and H-*y*″ (see Fig. 1 for numbering). COSY ^{1}H/^{1}H, ^{1}H/^{13}C NMR correlation (on Brucker AC 500 spectrometer), ^{13}C DEPT, and/or mass spectrometry data fully confirm the signal assignments and structure of the isolated materials. Electron-spray ionization mass spectra (ESI-MS) were run on a Finnigan MAT TSQ 7000 apparatus equipped with an atmospheric pressure ionization source. This method used in positive mode gives either M^+, $[M+H]^+$ and/or $[M+Na]^+$ signals.

The synthesis of 6-[2(*S*)-*tert*-butoxycarbonylamino-3-methyl-butyrylamino]-hexanoic acid, (Boc)ValNC5C(O) **1** was performed from *N*-Boc-(L)-valine, 6-amino-hexanoic acid using DCC/HOSu activation, according to literature [39]: R_f 0.36 (98:2 CH_2Cl_2–MeOH); ^{1}H NMR ($CDCl_3$): δ 9.76 (1H, bs, OH), 6.98 (1H, m, H-7″), 5.72 (1H, d, *J* 9.1 Hz, H-3′), 3.86 (1H, m, H-2′), 3.19 (2H, m, H-6″), 2.27 (2H, t, *J* 7.3 Hz, H-2″), 1.96 (1H, m, H-4′), 1.62–1.30 (6H, m, H-3″–H-5″), 1.37 [9H, s, $C(CH_3)_3$], 0.87 (6H, d, *J* 6.4 Hz, H-5′); ^{13}C NMR ($CDCl_3$): δ 177.4 (C-1″), 172.4 (C-1′), 156.4 [OC(O)NH], 79.9 [$C(CH_3)_3$], 60.7 (C-2′), 39.6 (C-6″), 34.3 (C-2″), 31.2 (C-4′), 29.4 (C-5″), 28.7 [$C(CH_3)_3$], 26.7 (C-4″), 24.8 (C-3″), 19.7 and 18.7 (C-5′).

6.1.2. Synthesis of protected Boc-valine prodrugs of protease inhibitors (condensation step)

6.1.2.1. Ind(8)–C(O)C5N(Boc)Val and Ind–[C(O)C5N(Boc)Val]$_2$. General esterification method: Compound **1** (270.3 mg, 0.82 mmol) and DMAP (39.4 mg, 0.32 mmol) were added to indinavir (506 mg, 0.75 mmol) in CH_2Cl_2 (10 mL). Then, EDC (372 mg, 1.95 mmol) was added to the mixture at 0 °C and the solution was stirred for 15 min at 0 °C then for 24 h at room temperature. The reaction mixture was diluted with CH_2Cl_2 and washed. The organic layer dried over Na_2SO_4 was filtered, and evaporated under reduced pressure. Then, the residue was chromatographed on silica gel (10:0 to 9.5:0.5 CH_2Cl_2–EtOH) to give Ind(8)–C(O)C5N(Boc)Val (300 mg, 20%) and Ind–[C(O)C5N(Boc)Val]$_2$ (360 mg, 18%) as white solids.

6.1.2.1.1. Ind(8)–C(O)C5N(Boc)Val. R_f 0.44 (98:2 CH_2Cl_2–MeOH); $t_R = 13.2$ min (gradient A); ^{1}H NMR ($CDCl_3$): δ 8.50 (2H, m, H-28, H-29), 7.61 (1H, d, *J* 7.7 Hz, H-26), 7.45 (1H, bs, H-21), 7.27 (1H, m, H-27), 7.21–7.11 (9H, m, H-2–H-5, H-32–H-36), 6.63 (1H, d, *J* 8.5 Hz, H-10), 6.52 (1H, bs, H-7″), 5.64 (1H, dd, *J* 5.3, *J* 9.0 Hz, H-9), 5.25 (1H, m, H-8), 5.18 (1H, d, *J* 8.9 Hz, H-3′), 3.86 (1H, m, H-14), 3.78 (1H, t, *J* 8.0 Hz, H-2′), 3.47 (2H, s, H-24), 3.12 (1H, dd, *J* 4.8, 17.1 Hz, H-7a), 3.06–3.00 (4H, m, H-6″, H-19, H-30a), 2.90 (1H, d, *J* 17.1 Hz, H-7b), 2.92–2.88 (1H, m, H-12), 2.83 (1H, t, *J* 8.6 Hz, H-18a), 2.70–2.47 (7H, m, H-15, H-16, H-17a, H-18b, H-30b), 2.41 (1H, t, *J* 8.2 Hz, H-17b), 1.97 (4H, m, H-4′, H-2″, H-13a), 1.50 (1H, m, H-13b), 1.40 [13H, m, H-3″, H-5″, $C(CH_3)_3$], 1.32 (9H, m, H-23), 1.18 (1H, m, H-4″a), 1.11 (1H, m, H-4″b), 0.88, 0.85 (6H, 2d, *J* 6.6 Hz, H-5′), ^{13}C NMR ($CDCl_3$): δ 174.9 (C-11), 172.5 (C-1′), 172.0 (C-1″), 169.8 (C-20), 155.9 [OC(O)NH], 150.4 (C-29), 149.0 (C-28), 140.9 (C-31), 139.8, 139.4 (C-1, C-6), 136.8 (C-26), 132.7 (C-25), 128.9 (C-32, C-36), 128.3 (C-33, C-35), 128.0 (C-2), 127.0, 126.3 (C-3, C-4), 125.0 (C-34), 123.7 (C-5), 123.5 (C-27), 79.8 [$C(CH_3)_3$], 76.0 (C-8), 66.2 (C-14), 65.0 (C-19), 61.6 (C-15), 60.3 (C-2′), 60.1 (C-24), 55.1 (C-9, C-16), 52.6 (C-17), 51.1 (C-22), 48.7 (C-18), 46.1 (C-12), 39.4 (C-30), 38.8 (C-13), 38.7 (C-6″), 37.6 (C-7), 33.9 (C-2″), 30.7 (C-4′), 29.0 (C-23), 28.6 (C-5″), 28.4 [$C(CH_3)_3$], 25.8 (C-4″), 24.0 (C-3″), 19.3, 18.1 (C-5′).

6.1.2.1.2. Ind–[C(O)C5N(Boc)Val]$_2$. R_f 0.52 (98:2 CH_2Cl_2–MeOH); $t_R = 20.6$ min (gradient A); ^{1}H NMR ($CDCl_3$): δ 8.48 (2H, m, H-28, H-29), 7.63 (1H, d, *J* 7.7 Hz, H-26), 7.21–7.18 (11H, m, H-2–H-5, H-21, H-27, H-32–H-36), 6.92 (2H, bs, H-7″), 6.77 (1H, d, *J* 8.5 Hz, H-10), 5.66 (1H, dd, *J* 5.3, *J* 8.5 Hz, H-9), 5.45–5.10 (4H, m, H-3′, H-8, H-14), 3.88 (2H, t, *J* 7.7 Hz, H-2′), 3.47 (2H, m, H-24), 3.13–2.04 (26H, m, H-4′, H-2″, H-6″, H-7, H-12, H-13, H-15–H-19, H-30), 1.43–1.11 [39H, m, H-23, H-3″–H-5″, $C(CH_3)_3$], 0.91 (12H, m, H-5′); ^{13}C NMR ($CDCl_3$): δ 174.3 (C-11), 173.6, 172.6 (C-1′), 171.8 (C-1″), 170.3 (C-20), 156.1 [OC(O)NH], 150.2 (C-29), 148.7 (C-28), 140.8 (C-31), 139.3, 139.1 (C-1, C-6), 136.8 (C-26), 133.0 (C-25), 128.8 (C-32, C-36), 128.4 (C-33, C-35), 128.0 (C-2), 127.1, 126.5 (C-3, C-4), 124.9 (C-34), 124.0 (C-5), 123.4 (C-27), 79.6 [$C(CH_3)_3$], 75.8 (C-8), 69.8 (C-14), 67.0 (C-19), 60.1 (C-2′), 59.9 (C-24), 58.9 (C-15), 55.2 (C-9), 55.7, 52.1 (C-16, C-17), 50.9 (C-22), 50.1 (C-18), 45.2 (C-12), 39.5 (C-30), 39.0 (C-6″, C-7), 37.5 (C-13), 34.3, 33.9 (C-2″), 30.9 (C-4′), 29.0 (C-23), 28.3 (C-5″), 28.4 [$C(CH_3)_3$], 26.4, 26.2 (C-4″), 24.6, 24.1 (C-3″), 19.3, 18.0 (C-5′).

6.1.2.2. Saq–C(O)C5N(Boc)Val. The general esterification method applied to **1** (250 mg, 0.75 mmol), DMAP (39.4 mg, 0.32 mmol), saquinavir (506 mg, 0.75 mmol), and EDC (172 mg, 0.9 mmol) in 10 mL CH_2Cl_2 afforded after work-up, and purification by chromatography on silica gel (10:0 to 9.8:0.2 $CHCl_3$–MeOH) Saq–C(O)C5N(Boc)Val (510 mg, 69%) as a white solid. R_f 0.50 (98:2 CH_2Cl_2–MeOH); $t_R = 19.7$ min (gradient A); ^{1}H NMR ($CDCl_3$–CD_3OD): δ 8.33 (1H, d, *J* 8.6 Hz, H-6), 8.04 (2H, m, H-1, H-7), 7.87 (1H, d, *J* 7.5 Hz, H-4), 7.71 (1H, m, H-2), 7.56 (1H, m, H-3), 7.14 (2H, m, H-21, H-25), 6.92 (2H, t, *J* 7.4 Hz, H-22, H-24), 6.77 (1H, m, H-23), 5.20 (1H, m, H-26), 4.87 (m, H-12, partially hidden by the signal of water), 4.34 (1H, m, H-18), 3.76–3.30 (2H, m, H-2′, H-37), 3.22–2.52 (8H, m, H-13, H-19, H-27, H-29), 2.66–2.52 (4H, m, H-30, H-35, H-36), 2.32–1.48 (19H, m, H-4′, H-2″–H-6″, H-31–H-34), 1.33 (9H, s, H-41), 1.24 [9H, s, $C(CH_3)_3$], 0.81 (6H, m, H-5′); ^{13}C NMR ($CDCl_3$–CD_3OD): δ 175.4 (C-1″), 174.9,

174.7 (C-14, C-16), 174.2 (C-1′), 172.2 (C-38), 165.9 (C-10), 157.7 [OC(O)NH], 150.1 (C-8), 147.7 (C-9), 139,1 (C-20), 138.8 (C-6), 131.4 (C-1), 130.7 (C-2, C-4), 130.1 (C-21, C-25), 129.4 (C-5), 129.2 (C-22, C-24), 128.9 (C-3), 127.1 (C-23), 119.5 (C-7), 80.4 [*C*(CH$_3$)$_3$], 74.4 (C-26), 70.6 (C-37), 61.6 (C-2′), 59.8 (C-29), 56.8 (C-27), 52.9 (C-12), 51.9 (C-40), 51.4 (C-18), 40.0 (C-6″), 37.9 (C-13), 36.8 (C-30), 35.5 (C-2″), 35.0 (C-19), 34.6 (C-35), 31.9 (C-4′), 29.0 (C-41), 28.7 [C(*C*H$_3$)$_3$], 31.7, 31.3, 27.3, 27.0, 25.9, and 25.3 (C-3″–C-5″, C-31–C-34, C-36), 19.8, 18.5 (C-5′).

6.1.2.3. Nelf(1)-C(O)C5N(Boc)Val and Nelf-[C(O)C5N(Boc)Val]$_2$. The general esterification method was applied to **1** (247 mg, 0.75 mmol), DMAP (135 mg, 0.90 mmol), nelfinavir (427 mg, 0.75 mmol) and EDC (173 mg, 0.90 mmol) in 10 mL DMF. After evaporation of DMF and extraction with AcOEt, the residue was purified by chromatography on silica gel (100:0–98:2 $CHCl_3$–EtOH) giving Nelf(1)–C(O)C5N(Boc)Val (198 mg, 30%) and Nelf–[C(O)C5N(Boc)Val]$_2$ (89 mg, 10%) as white solids.

6.1.2.3.1. Nelf(1)–C(O)C5N(Boc)Val. R_f 0.27 (98:2 $CHCl_3$–EtOH); $t_R = 21.95$ min (gradient A); ^{1}H NMR (CD_3OD): δ 7.54 (2H, d, J 7.5 Hz, H-13, H-17), 7.41 (1H, dd, J 7.6, J 0.9 Hz, H-4), 7.36–7.30 (2H, m, H-14, H-16), 7.31 (1H, t, $J \sim 7.9$ Hz, H-3), 7.25–7.22 (1H, m, H-15), 7.13 (1H, d, J 8.0 Hz, H-2), 4.51 (1H, m, H-10), 4.15 (1H, m, H-18), 3.88 (1H, d, J 6.7 Hz, H-2′), 3.60–3.49 (2H, m, H-11), 3.38–3.30 (1H, m, H-6″a), 3.29–3.23 (1H, m, H-6″b), 3.08 (1H, d, J 10.0 Hz, H-20a), 2.70–2.63 (4H, m, H-2″, H-19a, H-28), 2.30 (3H, s, H-7), 2.60–2.23 (2H, m, H19b, H-20b), 2.08–2.02 (1H, m, H-4′), 1.51 [9H, S, C(CH$_3$)$_3$], 1.88–1.25 (18H, m, H-3″–H-5″, H-21–H-27), 1.21 (9H, s, H-32), 1.00, 0.99 (6H, 2d, J 6.9 Hz, H-5′); ^{13}C NMR (CD_3OD): δ 176.2 (C-8), 174.3, 173.4 (C-1′, C-29), 172.3 (C-1″), 157.9 [OC(O)NH], 151.1 (C-1), 140.1 (C-5), 137.6 (C-12), 130.8 (C-13, C-17), 130.1 (C-14, C-16), 129.6 (C-6), 127.7 (C-3), 127.3 (C-15), 126.3 (C-4), 124.7 (C-2), 80.8 [*C*(CH$_3$)$_3$], 71.1 (C-28), 70.7 (C-18), 61.7 (C-2′), 60.6 (C-20), 59.8 (C-19), 54.7 (C-10), 52.1 (C-31), 40.3 (C-6″), 37.6 (C-21), 35.9 (C-11), 35.1 (C-26), 35.0 (C-2″), 32.2 (C-4′), 31.9 (C-27), 30.1 (C-5″), 29.2, 29.1 [C-32, C(*C*H$_3$)$_3$], 27.6 (C-4″), 25.8 (C-3″), 30.1, 27.2, and 21.9 (C-22–C-25), 18.8, 18.7 (C-5′), 13.9 (C-7).

6.1.2.2.2. Nelf–[C(O)C5N(Boc)Val]2. R_f 0.36 (98:2 $CHCl_3$–EtOH); $t_R = 26.60$ min (gradient A); ^{1}H NMR ($CDCl_3$): δ 7.77 (1H, d, J 8.9 Hz, NH), 7.40 (2H, d, J 7.5 Hz, H-13, H-17), 7.31 (1H, d, J 7.4 Hz, H-4), 7.24–7.21 (2H, m, H-14, H-16), 7.16–7.11 (2H, m, H-3, H-15), 6.97 (1H, d, J 8.0 Hz, H-2), 6.79 (1H, m, NH), 6.54 (1H, bs, NH), 5.82 (1H, s, NH), 5.36 (1H, m, H-18), 5.25 (2H, m, NH), 4.60 (1H, m, H-10), 3.84 (1H, m, H-2′), 3.62 (1H, m, H-11a), 3.42 (1H, m, H-11b), 3.29–3.03 (4H, m, H-6″), 2.96 (1H, d, J 10.6 Hz, H-20a), 2.59 (1H, m, H-19a), 2.52 (2H, t, J 7.5 Hz, H-2″), 2.40 (1H, m, H-28), 2.21 (2H, m, H-2″), 2.16 (3H, s, H-7), 2.11–1.89 (4H, m, H-4′, H-19b, H-20b), 1.39, 1.37 [18H, 2s, C(CH$_3$)$_3$], 1.74–1.12 (24H, m, H-3″–H-5″, H-21–H-27), 1.02 (9H, s, H-32), 0.90, 0.86 (6H, 2d, J 6.7 Hz, H-5′), 0.80 (6H, 2d, J 7.0 Hz, H-5′); ^{13}C NMR ($CDCl_3$): δ 174.2 (C-8), 172.6, 171.8, and 171.7 (C-1′, C-29), 171.4 169.4 (C-1″), 156.0, 155.9 [OC(O)NH], 149.6 (C-1), 138.9 (C-5), 135.8 (C-12), 129.8 (C-13, C-17), 128.9 (C-14, C-16), 128.2 (C-6), 126.3 (C-3), 126.2 (C-15), 124.9 (C-4), 123.2 (C-2), 79.7, 79.4 [*C*(CH$_3$)$_3$], 70.5, 70.3 (C-18, C-28), 60.1, 59.9 (C-2′), 59.5 (C-20), 55.9 (C-19), 51.3 (C-10), 51.1 (C-31), 39.1 (C-6″), 36.0 (C-21), 35.7 (C-11), 34.2, 34.0 (C-2″), 33.8 (C-26), 31.1 (C-4′), 31.0 (C-27), 29.2 (C-5″), 28.3 (C-32), [C(*C*H$_3$)$_3$], 26.4, 26.3 (C-4″), 24.5, 24.4 (C-3″), 29.0, 25.9, and 20.4 (C-22–C-25), 19.3, 18.0, 17.8 (C-5′), 13.0 (C-7).

6.1.3. Synthesis of valine prodrugs of protease inhibitors (deprotection step)

6.1.3.1. Ind(8)–C(O)C5NVal. General deprotection method: Ind(8)–C(O)C5N(Boc)Val (250 mg, 0.27 mmol) in a 1:9 TFA–CH_2Cl_2 v/v mixture (12 mL) was stirred for 4 h at 0 °C. The residue obtained after evaporation of the solvents was purified by chromatography (9:1 to 8:2 CH_2Cl_2–MeOH) to give Ind(8)–C(O)C5NVal (as its mono-TFA salt) (228 mg, 90%) as a white solid. R_f 0.34 (9:1 CH_2Cl_2–MeOH); $t_R = 9.3$ min (gradient A); ^{1}H NMR (CD_3OD): δ 8.57 (1H, m, H-29), 8.52 (1H, m, H-28), 7.96 (1H, d, J 7.9 Hz, H-26), 7.51 (1H, dd, J 5.1, J 7.9 Hz, H-27), 7.34–7.09 (9H, m, H-2–H-5, H-32–H-36), 5.52 (1H, d, J 10.1 Hz, H-9), 5.33 (1H, td, J 1.8, J 5.1 Hz, H-8), 4.05–3.45 (4H, m, H-2′, H-14, H-24), 3.26–2.60 (16H, m, H-6″, H-7, H-12, H-15–H-19, H-30), 2.11 (3H, m, H-4′, H-2″), 1.85 (1H, m, H-13a), 1.45–1.35 (7H, m, H-13b, H-3″–H-5″), 1.25 (9H, m, H-23), 0.97 (6H, d, J 6.8 Hz, H-5′); ^{13}C NMR (CD_3OD): δ 177.5 (C-11), 174.5 (C-1′, C-1″), 169.3 (C-20), 150.0 (C-29), 148.9 (C-28), 141.5 (C-31), 140.9, 140.5 (C-1, C-6), 140.8 (C-26), 133.5 (C-25), 130.1 (C-32, C-36), 129.5 (C-33, C-35), 129.3 (C-2), 128.2, 127.5 (C-3, C-4), 125.9 (C-34), 125.1 (C-5, C-27), 76.8 (C-8), 67.1 (C-14), 67.0 (C-19), 62.6 (C-15), 59.9 (C-2′), 59.0 (C-24), 56.7 (C-9), 54.4 (C-16, C-17), 52.7 (C-22), 50.9 (C-18), 45.8 (C-12), 40.6, 40.3 (C-6″, C-13, C-30), 38.2 (C-7), 34.7 (C-2″), 31.5 (C-4′), 29.9 (C-5″), 28.7 (C-23), 27.4 (C-4″), 25.4 (C-3″), 18.8, 18.1 (C-5′); ESI-MS (positive mode): *m/z* 826.7 $[M + H]^+$, 848.6 $[M + Na]^+$, in agreement with the calculated mass for [M] = $C_{47}H_{67}N_7O_6$ (825.52).

6.1.3.2. Ind–[C(O)C5NVal]$_2$. Deprotection of Ind–[C(O)C5N(Boc)Val]2 (300 mg, 0.24 mmol) afforded after purification by chromatography (9:1 to 8:2 CH_2Cl_2–MeOH) Ind–[C(O)C5NVal]$_2$ (as its di-TFA salt) (288 mg, 87%) as a white solid. R_f 0.23 (9:1 CH_2Cl_2–MeOH); $t_R = 9.1$ min (gradient A); ^{1}H NMR ($CDCl_3$–CD_3OD): δ 8.91 (2H, bs, H-28, H-29), 8.20 (1H, d, J 8.1 Hz, H-26), 7.94 (1H, s, H-21), 7.61–7.86 (10H, m, H-2–H-5, H-27, H-32–H-36), 6.07 (1H, d, J 5.2 Hz, H-9), 5.83 (1H, m, H-8), 5.58 (1H, m, H-14), 3.98 (1H, m, H-2′), 3.81–3.60 (4H, m, H-7, H-24), 3.57–2.45 (23H, m, H-4′, H-2″, H-6″, H-12, H-13, H-15–H-19, H-30), 2.12–1.66 (23H, m, H-3″–H-5″, H-23), 1.44–1.34 (12H, m,

H-5′); ^{13}C NMR ($CDCl_3$-CD_3OD): δ 175.2 (C-11), 173.7 (C-1′), 173.2 (C-1″), 170.8 (C-20), 149.4 (C-29), 147.8 (C-28), 140.3 (C-31), 139.2, 138.7 (C-1, C-6), 137.5 (C-26), 133.2 (C-25), 128.6 (C-32, C-36), 128.2 (C-33, C-35), 127.9 (C-2), 126.9, 126.3 (C-3, C-4), 124.7 (C-34), 123.7 (C-5, C-27), 75.6 (C-8), 69.5 (C-14) 66.8 (C-19), 59.6 (C-2′), 59.4 (C-24), 58.3 (C-15), 55.0 (C-9), 55.3, 51.7 (C-16, C-17), 50.8 (C-22), 49.9 (C-18), 44.2 (C-12), 39.3 (C-30), 38.7 (C-6″, C-7), 37.1 (C-13), 33.9, 33.6 (C-2″), 31.0 (C-4′), 28.7, 28.6 (C-5″), 28.2 (C-23), 26.1, 26.0 (C-4″), 24.2, 23.9 (C-3″), 18.7, 16.6 (C-5′); ESI-MS (positive mode): *m/z* 1039.0 $[M+H]^+$, 1061.7 $[M+Na]^+$, in agreement with the calculated mass for $[M] = C_{58}H_{87}N_9O_8$ (1037.67).

6.1.3.3. Saq–C(O)C5NVal. Deprotection of Saq–C(O)C5N(-Boc)Val (350 mg, 0.36 mmol) afforded Saq–C(O)C5NVal (as its tri-TFA salt) (400 mg, 92%) as a white solid. R_f 0.59 (9:1 CH_2Cl_2–MeOH), HPLC: $t_R = 14.4$ min; ^{1}H NMR (CD_3OD): δ 8.45 (1H, d, *J* 8.5 Hz, H-6), 8.14 (1H, d, *J* 8.5 Hz, H-7), 8.10 (1H, d, *J* 7.1 Hz, H-1), 7.97 (1H, d, *J* 8.2 Hz, H-4), 7.81 (1H, td, *J* 1.5, *J* 7.7 Hz, H-2), 7.67 (1H, td, *J* 7.5, *J* 1.20 Hz, H-3), 7.16 (2H, d, *J* 7.2 Hz, H-21, H-25), 6.98 (2H, t, *J* 7.4 Hz, H-22, H-24), 6.83 (1H, m, H-23), 5.31 (1H, m, H-26), 4.87 (m, H-12, partially hidden by the signal of water), 4.45 (1H, m, H-18), 3.62–3.52 (2H, m, H-2′, H-37), 3.33–2.90 (8H, m, H-13, H-19, H-27, H-29), 2.74–2.65 (4H, m, H-30, H-35, H-36), 2.36 (2H, t, *J* 7.2 Hz, H-2″), 2.18–1.45 (17H, m, H-4′, H-3″–H-6″, H-31–H-34), 1.33 (9H, s, H-41), 0.81 (6H, m, H-5′); ^{13}C NMR (CD_3OD): δ 174.9 (C-1″), 174.7 (C-16), 173.3 (C-14), 172.8 (C-1′), 169.3 (C-38), 166.2 (C-10), 150.2 (C-9), 147.9 (C-20), 139.0 (C-7), 139.3 (C-8), 131.6 (C-2), 130.9 (C-5), 130.7 (C-1), 130.1 (C-21, C-25), 129.5 (C-3), 129.3 (C-22, C-24), 129.1 (C-4), 127.4 (C-23), 119.6 (C-6), 73.7 (C-26), 66.8 (C-37), 59.9 (C-2′), 57.3 (C-27, C-29), 53.2 (C-12), 52.4 (C-40), 51.6 (C-18), 40.4 (C-6″), 37.8 (C-13), 36.3 (C-19), 36.1 (C-30), 34.8 (C-2″), 34.0 (C-35), 31.5 (C-4′), 28.9 (C-41), 30.8, 30.0, 27.4, 26.9, 26.6, and 25.3 (C-3″–C-5″, C-31–C-34, C-36), 18.9, 18.0 (C-5′); ESI-MS (positive mode): *m/z* 883.8 $(M+H)^+$, 905.6 $(M+Na)^+$, in agreement with the calculated mass for $[M] = C_{49}H_{70}N_8O_9$ (882.54).

6.1.3.4. Nelf(1)–C(O)C5NVal. Deprotection of Nelf(1)–C(O)C5N(Boc)Val (150 mg, 0.17 mmol) afforded after purification by chromatography (1:0 to 9:1 CH_2Cl_2–MeOH) Nelf(1)–C(O)C5NVal (as its mono-TFA salt) 150 mg (98%) as a white solid. R_f 0.32 (9:1 $CHCl_3$–MeOH); $t_R = 14.44$ min (gradient A); ^{1}H NMR (CD_3OD): δ 7.45 (2H, d, *J* 7.5 Hz, H-13, H-17), 7.31–7.00 (6H, m, H-2–H-4, H-14–H-16), 4.40 (1H, m, H-10), 4.05 (1H, m, H-18), 3.60–2.95 (6H, m, H-2′, H-6″, H-11, H-20a), 2.64–2.48 (4H, m, H-2″, H-19a, H-28), 2.17 (3H, s, H-7), 2.30–1.88 (3H, m, H-4′, H-19b, H-20b), 1.80–1.14 (18H, m, H-3″–H-5″, H-21–H-27), 1.10 (9H, s, H-32), 0.95, 0.92 (6H, 2d, *J* 6.8 Hz, H-5′); ^{13}C NMR (CD_3OD): δ 176.2 (C-8) 173.2, 173.1 (C-1′, C-29), 172.3 (C-1″), 151.1 (C-1), 140.2 (C-5), 137.7 (C-12), 130.0 (C-13, C-17), 130.0 (C-14, C-16), 129.4 (C-6), 127.6 (C-3), 127.0 (C-15), 126.2 (C-4), 124.6 (C-2), 71.0 (C-28), 70.4 (C-18), 60.8 (C-2′), 60.4 (C-20), 59.6 (C-19), 54.4 (C-10), 51.9 (C-31), 40.2 (C-6″), 37.6 (C-21), 35.3 (C-11), 35.2 (C-26), 34.7 (C-2″), 32.5 (C-4′), 32.1 (C-27), 30.0 (C-5″), 28.8 (C-32), 27.5 (C-4″), 25.6 (C-3″), 31.7, 27.1, and 21.7 (C-22–C-25), 19.3, 17.9 (C-5′), 13.5 (C-7); ESI-MS (positive mode): *m/z* 780.6 $(M+H)^+$, in agreement with the calculated mass for $[M] = C_{43}H_{65}N_5O_6S$ (779.47).

6.1.3.5. Nelf–[C(O)C5NVal]2. Deprotection of Nelf–[C(O)C5N(Boc)Val]2 (60 mg, 0.05 mmol) afforded after purification by chromatography (1:0 to 85:15 CH_2Cl_2–MeOH) Nelf–[C(O)C5NVal]2 (as its di-TFA salt) (58 mg, 95%) as a white solid. R_f 0.22 (9:1 $CHCl_3$–EtOH); $t_R = 13.47$ min (gradient A); ^{1}H NMR (CD_3OD): δ 7.58 (2H, m, H-13, H-17), 7.32–7.20 (6H, m, H-3, H-4, H-14–H-16), 7.06 (1H, m, H-2), 5.52 (1H, m, H-18), 4.53 (1H, m, H-10), 3.75 (1H, m, H-2′), 3.53 (2H, dd, *J* 6.1, *J* 8.2 Hz, H-11), 3.40–3.08 (6H, m, H-6″, H-19a, H-20a), 2.93 (2H, m, H-2″), 2.60 (1H, t, *J* 7.2 Hz, H-28), 2.38 (2H, m, H-2″), 2.16 (3H, s, H-7), 2.20–1.20 (28H, m, H-4′, H-3″–H-5″, H-19b, H-20b, H-21–H-27), 1.27 (9H, s, H-32), 0.96, 0.99 (12H, 2d, *J* 6.9 Hz, H-5′); ^{13}C NMR (CD_3OD): δ 174.3 (C-8), 173.3, 172.6 (C-1′, C-29), 169.4, 168.6 (C-1″), 151.2 (C-1), 139.6 (C-5), 136.1 (C-12), 131.8 (C-13, C-17), 130.3 (C-14, C-16), 129.3 (C-6), 128.2 (C-3), 127.8 (C-15), 125.8 (C-4), 124.9 (C-2), 72.1 (C-18, C-28), 59.9 (C-2′), 57.8 (C-19, C-20), 52.8 (C-31), 51.7 (C-10), 40.4 (C-6″), 35.5 (C-21), 35.2 (C-11), 34.7, 34.6 (C-2″), 33.0 (C-26), 31.5 (C-4′), 29.9 (C-5″, C-27), 28.7 (C-32), 27.5 (C-4″), 25.6 (C-3″), 31.5, 29.9, 27.5, and 25.1 (C-22–C-25), 18.8, 18.0 (C-5′), 13.5 (C-7); ESI-MS (positive mode): *m/z* 992.8 $(M+H)^+$, in agreement with the calculated mass for $[M] = C_{54}H_{85}N_7O_8S$ (991.62).

6.2. Biological assays

6.2.1. General methods, reagents and starting materials

1-Pentanesulfonic acid sodium salt, sodium acetate trihydrate, and acetonitrile were high-performance liquid chromatography (HPLC) grade. Foetal bovine serum (FBS), Dulbecco's phosphate buffered saline (DPBS), penicillin:-streptomycin solution (5000 U/mL:5000 μg/mL), trypsin–EDTA 0.25% solution (2.5 g trypsin and 0.2 g EDTA in 1 L DPBS), D-(+)-glucose, and *N*-[2-hydroxyethyl]piperazine-*N*-ethanesulfonic acid (HEPES) were purchased from Sigma Chemical (St Quentin Fallavier, France). Dulbecco's modified eagle's medium (DMEM) and nonessential aminoacids DMEM 100 × (NEAA) were purchased from Gibco-Life Technologies (Cergy-Pontoise, France). Transport Medium (TM) consisted of DPBS containing 25 mM glucose and 10 mM HEPES (pH 7.4). Cell culture medium consisted of DMEM supplemented with 20% foetal bovine serum, 1% NEAA, and 2% penicillin–streptomycin.

6.2.2. HPLC conditions

All HPLC analyses used for chemical stability and transport experiments were performed using a HP1100 apparatus

with a Lichrospher 100 RP-18 (5 μm)-packed column (250 × 3.2 mm) with a flow rate of 1 mL/min. The isocratic mobile phase consisted of $CH_3COONa \cdot 3H_2O$ (15 mM) and $CH_3(CH_2)_4SO_3Na$ (15 mM), 5 mM pH 6 buffer and CH_3CN: 59:41 for indinavir, Ind(8)–C(O)C5NVal and Ind–[C(O)C5NVal]2, 41:59 for saquinavir and Saq–C(O)C5NVal, and 45:55 for nelfinavir, Nelf(1)–C(O)C5NVal and Nelf–[C(O)C5NVal]2. The prodrugs and/or drugs were detected by measuring their UV absorption at 210 nm (indinavir, nelfinavir and their derivatives) or 254 nm (saquinavir and its derivative) and the signals (peak integration) were interpreted by the software provided. Under their respective HPLC conditions, the retention times measured for the different compounds were of 10.4 min for indinavir, 10.0 min for Ind(8)–C(O)C5NVal, 7.0 min for Ind–[C(O)C5NVal]2, 5.7 min for saquinavir, 4.3 min for Saq–C(O)C5NVal, 12.5 min for nelfinavir, 10.9 min for Nelf(1)–C(O)C5NVal, 8.2 min for Nelf–[C(O)C5NVal]2. The prodrug and/or drug concentration was determined from HPLC calibration curves. These curves were established under the same HPLC conditions, using standard calibrated prodrug and drug solutions that were prepared in the same hydrolysis medium as the sample under investigation. The calibration curves were linear (correlation coefficients from 0.9993 to 0.9998) in a concentration range of 0.4 to 1000 μM for indinavir and its prodrugs, 0.1 to 200 μM for saquinavir and its prodrugs, and 0.1 to 310 μM for nelfinavir and its prodrugs, the lower limit corresponding to the limit of detection that can be quantified with accuracy. Above the lower concentration limit, the analytical method was reproducible.

6.2.3. Hydrolysis

Hydrolysis experiments were performed by incubating 20 mL of a DMEM–MeOH solution (pH 7.3) of the prodrug (250 μg/mL) at 37 °C with stirring. The amount of MeOH (v/v) in these solutions was 3% for Ind(8)–C(O)C5NVal, 2% for Ind–[C(O)C5NVal]2, 4% for Saq–C(O)C5NVal, 5% for Nelf(1)–C(O)C5NVal and 3% for Nelf–[C(O)C5NVal]2. Hydrolysis was followed by HPLC monitoring of the disappearance of the prodrug and appearance of the parent PI by injecting 40 μL of the solution onto the HPLC column (for HPLC conditions see above). Plots of $\ln([\text{prodrug}]_o - [\text{prodrug}(t)])$ and of $\ln[\text{PI}(t)]$ against time were linear within the concentration range studied, indicating that the hydrolysis is a first order process with respect to the prodrug. The half-lives of hydrolysis ($t_{1/2}$) were measured, when possible, or calculated from these plots; $t_{1/2}$ is related to the slope, K, of these curves by the relation $t_{1/2} = (\ln 2)/K$.

6.2.4. Caco-2 cell culture

Caco-2 cells, clone TC7, were kindly provided by Dr. A. Zweibaum (INSERM U178, Villejuif, France). The cells were routinely maintained in 75 cm^2 culture flasks at 37 °C in an atmosphere containing 5% CO_2 and 95% relative humidity. Cells were split every 7 days at a density of 1.5×10^6 cells/flask. For the transepithelial transport experiments, Caco-2 cells (passage 60–65) were harvested with trypsin–EDTA and seeded on Anopore membrane inserts (0.2 μm pore diameter, 25 mm diameter; Nunc, Roskilde, Denmark) at a density of 5×10^5 cells/insert (cm^2). Apical (AP) and basolateral (BL) chamber volumes were maintained at 2 mL. Culture medium was changed every 3 to 4 days and cells were used for the experiments between days 14 and 27 post-seeding. Monolayer formation was monitored by measurement of transepithelial electrical resistance (TEER) using a Millicel ERS apparatus (Millipore).

6.2.5. Transport experiments

Before the transepithelial transport experiments, the Caco-2 monolayers were rinsed twice with the transport medium (TM) (both chambers) and pre-incubated for 30 min in the TM. After this equilibration period, the monolayer integrity was checked by measuring its TEER. For the transport experiments, only monolayers displaying TEER values above 176 Ω cm^2 and for which TEER values fell by less than 15% from the value measured at the end of the equilibration period were used. Under these conditions, the age of the cell monolayer within the 14 to 27 days post-seeding range did not affect the transport results. Transport was initiated by replacing the TM in the AP or in the BL "donor" compartment with 2 mL of the PI or prodrug solution. AP and BL chamber volumes were maintained at 2 mL. The test solutions were prepared by mixing a known amount of TM with a concentrated MeOH stock solution of the PI or prodrug under investigation to reach a final concentration of the PI or prodrug in the 150–185 μM, 26.5 μM, and 195–248 μM range for the indinavir, saquinavir, and nelfinavir derivatives, respectively (the exact concentrations used for each derivative are given in the figures showing their transepithelial transport). The final MeOH concentration in the PI or prodrug solutions in contact with the monolayers never exceeded 3% MeOH (TEER monitoring and transport experiments have shown that MeOH at concentrations up to 5% neither affected cell monolayer integrity during the 3-h period of transport experiment nor the amount of PI and/or prodrug transported, respectively). Two hundred microliters of samples were withdrawn from the "acceptor" compartment (opposite to the addition "donor" chamber) every 1 h over a period of 3 h and replaced by the same amount of fresh transport medium in order to maintain the same volume. The dilution was taken into account for the calculations. To prevent hydrolysis of the prodrugs, all these samples were stored at 4 °C awaiting for prodrug and/or parent PI HPLC-analysis (see Section 6.2.2). At the end of the experiments (3 h), samples were also taken from the "donor" compartment for HPLC analysis and the monolayers were checked for integrity by measuring TEER values. The concentrations of the prodrug and parent PI that were measured in the donor and acceptor chamber at the end of the transport experiment indicated that no non-specific adsorption on glass or on plastic had occurred. The experiments for which TEER has decreased by more than 8% from the value

measured at the beginning of the experiment were discarded. Transport was expressed as a percentage of the initial amount added to the donor compartment. All flux experiments were conducted at least in triplicate in the AP to BL and BL to AP directions. If possible, a concentration of the prodrug in the donor chamber the closest to that of the parent PI was privileged but solubility issues of the prodrug (which needed in some cases the use of MeOH) and detection issues of the prodrug and/or parent PI in the acceptor chamber was also considered for the selection of the prodrug concentration.

6.2.6. Data analysis for the transport experiments

The apparent permeability coefficients P_{app} (cm/s) were calculated by linear regression analysis on the time course plot of amount of (pro)drug transported from equation $P_{app} = k^*(V_D/A)$, where k is the slope of the linear curve $\ln(C_t/C_o) = -kt$, C_t being the (pro)drug concentration in the receiver chamber at time t, C_o the initial concentration in the donor chamber, A the membrane surface area (4.52 cm^2) and V_D the volume of the donor chamber (2 cm^3). These calculations were performed for each transport experiment and the values reported in Table 3 represent the means (±SD) of at least three independent experiments.

6.2.7. In vitro antiviral and cytotoxicity assays

The in vitro antiviral activity and cytotoxicity assays were performed according to published procedures [45–47]. Briefly, CEM-SS cells were infected with a dose of HIV-1 (LAI strain) infecting 50% of the cells. Four days later, the growth of HIV-1 was evaluated by measuring the reverse transcriptase (RT), which expresses the presence of the virus in the supernatant culture medium. The tested compounds were added to the cell cultures after viral infection. RT inhibition% was measured in comparison with the non-treated cells. The growth of HIV-1 [HTLV-I (IIIB)] was followed by the cytopathogenic effect induced by the virus in MT4 cells. MT4 cells were infected with a virus dose allowing 4 days later the death of 90%. The tested compounds were added in the cell culture medium after viral infection and cell viability was measured by the colorimetric MTT [3-(4,5-dimethylthiazol-2-yl)-2,5-diphenyl-2*H*-tetrazolium bromide] test. The percentage of protection was calculated as the ratio Δ.

$\Delta = [(\text{OD of treated infected cells} - \text{OD of untreated infected cells})/(\text{OD of non-infected cells} - \text{OD of untreated infected cells})] \times 100$.

The prodrug EC_{50} values were determined from the curves of the RT inhibition % (CEM-SS cells) or the protection percentage Δ (MT4 cells) against prodrug concentration. The effect of the prodrugs on cell viability was measured on non-infected cells using the colorimetric MTT test after 5 days of incubation at 37 °C with various concentrations of the tested product.

Acknowledgements

We thank the Fondation de la Recherche Médicale (Sidaction), the Agence Nationale de la Recherche sur le SIDA (ANRS), and the Centre National de la Recherche Scientifique (CNRS) for financial support, and the Conseil Régional de la Martinique for grant (D.R.).

References

[1] R.M. Gulick, Infect. Dis. Ther. 25 (2002) 179–236.
[2] A. Winston, M. Boffito, J. Antimicrob. Chemother. 56 (2005) 1–5.
[3] T.-W. Chun, L. Stuyver, S.B. Mizell, L.A. Ehler, J.A.M. Mican, M. Baseler, A.L. Lloyd, M.A. Nowak, A.S. Fauci, Proc. Natl. Acad. Sci. U.S.A. 94 (1997) 13193–13197.
[4] T.-W. Chun, A.S. Fauci, Proc. Natl. Acad. Sci. U.S.A. 96 (1999) 10958–10961.
[5] J.N. Blankson, D. Persaud, R.F. Siliciano, Annu. Rev. Med. 53 (2002) 557–593.
[6] X. Li, W.K. Chan, Adv. Drug Deliv. Rev. 39 (1999) 81–103.
[7] S. Taylor, A. Pereira, HIV Med. 1 (2000) 18–22.
[8] R.G. Jain, E.S. Furfine, L. Pedneault, A.J. White, J.M. Lenhard, Antiviral Res. 51 (2001) 151–177.
[9] S.K. Gan, K. Samaras, A. Carr, D. Chisholm, Diabetes Obes. Metab. 3 (2001) 67–71.
[10] P.W. Hruz, H. Murata, M. Mueckler, Am. J. Physiol. 280 (2001) E549–E553.
[11] M.J. Glesby, Infect. Dis. Ther. 25 (2002) 237–256.
[12] H. Murata, P.W. Hruz, M. Mueckler, Curr. Drug Targets: Infect. Disord. 2 (2002) 1–8.
[13] C.W. Flexner, Infect. Dis. Ther. 25 (2002) 139–159.
[14] A. Farese-Di Giorgio, M. Rouquayrol, J. Greiner, A.-M. Aubertin, P. Vierling, R. Guedj, Antivir. Chem. Chemother. 11 (2000) 97–110.
[15] M. Rouquayrol, B. Gaucher, J. Greiner, A.-M. Aubertin, P. Vierling, R. Guedj, Carbohydr. Res. 336 (2001) 161–180.
[16] M. Rouquayrol, B. Gaucher, D. Roche, J. Greiner, P. Vierling, Pharm. Res. 19 (2002) 1704–1712.
[17] P. Vierling, J. Greiner, Curr. Pharm. Des. 9 (2003) 1755–1770.
[18] B. Gaucher, M. Rouquayrol, D. Roche, J. Greiner, A.-M. Aubertin, P. Vierling, Org. Biomol. Chem. 2 (2004) 345–357.
[19] M. de Oliveira, J.-C. Olivier, C. Pariat, D. Roche, J. Greiner, P. Vierling, W. Couet, J. Pharm. Pharmacol. 57 (2005) 453–458.
[20] D. Roche, J. Greiner, A.M. Aubertin, P. Vierling, Bioconjug. Chem. 17 (2006) 1568–1581.
[21] G. Bold, A. Faessler, M. Lang, Eur. Pat., 594,540, 1994.
[22] K.Y. Hostetler, D.D. Richman, E.A. Forssen, L. Selk, R. Basava, M.F. Gardner, S. Parker, C. Basava, Biochem. Pharmacol. 48 (1994) 1399–1404.
[23] J. Alexander, D. Bindra, B.D. Dorsey, A.J. Repta, J.P. Vacca, PCT Int. Appl., 9514016, 1995.
[24] T. Cynkowski, G. Cynkowska, P.A. Crooks, H. Guo, P. Ashton, Abstr. Pap.- Am. Chem. Soc. 216 (1998) (MEDI-346).
[25] R.D. Tung, M.R. Hale, C.T. Baker, E.S. Furfine, I. Kaldor, W.W. Kazmierski, A. Spaltenstein, PCT Int. Appl., 9933815, 1999.
[26] W.M. Kazmierski, P. Bevans, E. Furfine, A. Spaltenstein, H. Yang, Bioorg. Med. Chem. Lett. 13 (2003) 2523–2526.
[27] T. Calogeropoulou, A. Detsi, E. Lekkas, M. Koufaki, Curr. Top. Med. Chem. 3 (2003) 1467–1495.
[28] S. Gunaseelan, O. Debrah, L. Wan, M.J. Leibowitz, A.B. Rabson, S. Stein, P.J. Sinko, Bioconjug. Chem. 15 (2004) 1322–1333.
[29] R. Jain, S. Agarwal, S. Majumdar, X. Zhu, D. Pal, A.K. Mitra, Int. J. Pharm. 303 (2005) 8–19.
[30] D.A. Degoey, W.J. Flosi, D.J. Grampovnik, L.L. Klein, D.J. Kempf, X.C. Wang, PCT Int. Appl., 2006014282, 2006.
[31] S. Luo, V.S. Kansara, X. Zhu, N.K. Mandava, D. Pal, A.K. Mitra, Mol. Pharm. 3 (2006) 329–339.

[32] J.M. Gatell, J. HIV Ther. 6 (2001) 95–99.
[33] L.A. Sorbera, L. Martin, J. Castaner, R.M. Castaner, Drugs Future 26 (2001) 224–231.
[34] T.M. Chapman, G.L. Plosker, C.M. Perry, Drugs 64 (2004) 2101–2124.
[35] S. Becker, L. Thornton, Expert Opin. Pharmacother. 5 (2004) 1995–2005.
[36] E.S. Furfine, C.T. Baker, M.R. Hale, D.J. Reynolds, J.A. Salisbury, A.D. Searle, S.D. Studenberg, D. Todd, R.D. Tung, A. Spaltenstein, Antimicrob. Agents Chemother. 48 (2004) 791–798.
[37] M.F. Fromm, Int. J. Clin. Pharmacol. Ther. 38 (2000) 69–74.
[38] B. Testa, J.M. Mayer, Hydrolysis in Drug and Prodrug Metabolism: Chemistry, Biochemistry, and Enzymology, Wiley-VCH, Zürich, Switzerland, 2003.
[39] A. Losse, Tetrahedron 29 (1973) 1203–1208.
[40] M. Bodanszky, A. Bodanszky, The Practice of Peptide Synthesis, Springer Verlag, Berlin, Germany, 1984.
[41] E. Breitmaier, W. Voelter, Carbon-13 NMR Spectroscopy, , In: Monographs in Modern Chemistry, vol. 5, Verlag Chemie, Weinheim, Germany, 1974.
[42] M. Hesse, H. Meier, B. Zeeh, Spectroscopic Methods in Organic Chemistry, Thieme, Stuttgart, Germany, 1995.
[43] U. Sequin, Helv. Chim. Acta 64 (1981) 2654–2664.
[44] I.I. Schuster, J. Org. Chem. 50 (1985) 1656–1662.
[45] R. Pauwels, J. Balzarini, M. Baba, R. Snoeck, D. Schols, P. Herdewijn, J. Desmyter, E. De Clercq, J. Virol. Methods 20 (1988) 309–321.
[46] C. Genu-Dellac, G. Gosselin, F. Puech, J.C. Henry, A.M. Aubertin, G. Obert, A. Kirn, J.L. Imbach, Nucleosides Nucleotides 10 (1991) 1345–1376.
[47] C. Moog, A. Wick, P. Le Ber, A. Kirn, A.-M. Aubertin, Antiviral Res. 24 (1994) 275–288.
[48] M.L. West, D.P. Fairlie, Trends Pharmacol. Sci. 16 (1995) 67–74.
[49] F. Lebon, M. Ledecq, Curr. Med. Chem. 7 (2000) 455–477.
[50] R.B. Kim, M.F. Fromm, C. Wandel, B. Leake, A.J.J. Wood, D.M. Roden, G.R. Wilkinson, J. Clin. Invest. 101 (1998) 289–294.
[51] B.J. Aungst, N.H. Nguyen, J.P. Bulgarelli, K. Oates-Lenz, Pharm. Res. 17 (2000) 1175–1180.
[52] P. Artursson, Crit. Rev. Ther. Drug Carrier Syst. 8 (1991) 305–330.
[53] P. Augustijns, P. Annaert, P. Heylen, G. Van den Mooter, R. Kinget, Int. J. Pharm. 166 (1998) 45–53.
[54] P. Annaert, G. Gosselin, A. Pompon, S. Benzaria, G. Valette, J.L. Imbach, L. Naesens, S. Hatse, E. De Clercq, G. Van Den Mooter, R. Kinget, P. Augustijns, Pharm. Res. 15 (1998) 239–245.
[55] M.-C. Gres, B. Julian, M. Bourrie, V. Meunier, C. Roques, M. Berger, X. Boulenc, Y. Berger, G. Fabre, Pharm. Res. 15 (1998) 726–733.
[56] P. Artursson, K. Palm, K. Luthman, Adv. Drug Deliv. Rev. 46 (2001) 27–43.
[57] J. Alsenz, H. Steffen, R. Alex, Pharm. Res. 15 (1998) 423–428.
[58] S.D. Ucpinar, S. Stavchansky, Biomed. Chromatogr. 17 (2003) 21–25.
[59] S. Lu, A.W. Gough, W.F. Bobrowski, B.H. Stewart, J. Pharm. Sci. 85 (1996) 270–273.
[60] B. Bhhatarai, R. Garg, Bioorg. Med. Chem. 13 (2005) 4078–4084.